COMPARATIVE STUDY BETWEEN PI, RST AND SLIDING MODE CONTROLLERS OF A DFIG-BASED WIND TURBINE

Ahmed. BOUROUINA   **Abdelkader CHAKER**

Electrical Engineering Department ENP Oran, Algeria,
Simulation, Commanded, Analysis and Maintenance Electrical Network.,
ahmed_bourouina@yahoo.fr   chakeraa@yahoo.fr

Abdelkaber Djahbar   **Zinelaabidine Boudjema**

Laboratoire Génie Electrique et Energies Renouvelables (LGEER), Electrical Engineering Department,
Hassiba Benbouali University, Chlef, Algeria.
a_djahbar @yahoo.fr   boudjemaa1983@yahoo.fr

Abstract: This paper deals with a variable speed device to produce electrical energy on a power network, based on a doubly-fed induction generator (DFIG) used in wind energy conversion systems. In the first place, we developed a model of the doubly fed induction generator. In order to control the power flowing between the stator of the DFIG and the power network, a control law is synthesized using three types of controllers: PI, RST and super twisting sliding mode controllers. Their respective performances are compared in terms of power reference tracking, response to sudden speed variations, sensitivity to perturbations and robustness against machine parameters variations.

Key words: Doubly fed induction generator, wind turbine, PI, RST, super twisting sliding mode.

1. Introduction

Wind energy is the most promising renewable source of electrical power generation for the future. Many countries promote the wind power technology through various national programs and market incentives. Wind energy technology has evolved rapidly over the past three decades with increasing rotor diameters and the use of sophisticated power electronics to allow operation at variable speed [1]. Doubly fed induction generator is one of the most popular variable speed wind turbines in use nowadays. As it's shown in Figure.1, this generator enables to obtain variable speed operations with a lower rated power converter. The stator is directly connected to the grid and the rotor is fed to magnetize the machine.

In recent years, dozens of work was done by researchers on the control of DFIG using a simplified model of the latter by negligence the stator resistance. This assumption, although it has been proven that it is a realistic approximation for medium power machines used in wind energy conversion, but in reality, the model does not reflect reality because this parameter still exists and it cannot be neglected. To overcome this drawback, in this work and in contrast to previous work, we used a real model of DFIG, i.e without negligence in this resistance.

A lot of works have been presented with diverse control diagrams of DFIG. These control diagrams are usually based on vector control notion with conventional PI controllers as proposed by Pena et al. in [2, 3]. The similar conventional controllers are also used to realize control techniques of DFIG when grid faults appear like unbalanced voltages [4, 5] and voltage dips [6]. It has also been shown in [7, 8] that glimmer problems could be resolved with suitable control strategies. Many of these works prove that stator reactive power control can be an adapted solution to these diverse problems.

In recent years, the sliding mode control (SMC) methodology has been widely used for robust control of nonlinear systems. Sliding mode control, based on the theory of variable structure systems (VSS), has attracted a lot of research on control systems for the last two decades. It achieves robust control by adding a discontinuous control signal across the sliding surface, satisfying the sliding condition. Nevertheless, this type of control has an essential disadvantage, which is the chattering phenomenon caused by the discontinuous control action. To treat these difficulties, several modifications to the original sliding control law have been proposed, the most popular being the boundary layer approach [8].

One way to improve sliding mode controller performance is to use a super twisting sliding mode controller (STSMC).

This paper discusses the control of electrical power exchanged between the stator of the DFIG and the power network by controlling independently the active and reactive power. After modelling the DFIG and choosing the appropriate *d-q* reference frame, active and reactive powers are controlled using three types of controllers: Integral-Proportional (PI), an RST controller based on pole placement theory PI and super twisting sliding mode. Their performances

are compared in terms of reference tracking, sensitivity to perturbations and robustness against machine's parameters variations.

2. The DFIG model

The application of Concordia and Park's transformation to the three-phase model of the DFIG permits to write the dynamic voltages and fluxes equations in an arbitrary d–q reference frame:

$$\begin{cases} V_{ds} = R_s I_{ds} + \dfrac{d}{dt}\psi_{ds} - \omega_s\psi_{qs} \\ V_{qs} = R_s I_{qs} + \dfrac{d}{dt}\psi_{qs} + \omega_s\psi_{ds} \\ V_{dr} = R_r I_{dr} + \dfrac{d}{dt}\psi_{dr} - \omega_r\psi_{qr} \\ V_{qr} = R_r I_{qr} + \dfrac{d}{dt}\psi_{qr} + \omega_r\psi_{dr} \end{cases}, \begin{cases} \psi_{ds} = L_s I_{ds} + M I_{dr} \\ \psi_{qs} = L_s I_{qs} + M I_{qr} \\ \psi_{dr} = L_r I_{dr} + M I_{ds} \\ \psi_{qr} = L_r I_{qr} + M I_{qs} \end{cases} \quad (1)$$

The stator and rotor angular velocities are linked by the following relation : $\omega_s = \omega + \omega_r$.

This electrical model is completed by the mechanical equation:

$$C_{em} = C_r + J\frac{d\Omega}{dt} + f\Omega \quad (2)$$

Where the electromagnetic torque C_{em} can be written as a function of stator fluxes and rotor currents :

$$C_{em} = p\frac{M}{L_s}(\psi_{qs}I_{dr} - \psi_{ds}I_{qr}) \quad (3)$$

3. Control strategy of the DFIG

In order to easily control the production of electricity by the wind turbine, we will carry out an independent control of active and reactive powers by orientation of the stator flux. This orientation will be made in this work with a real model of the DFIG, i.e. without negligence of the stator resistance [9, 10].

By choosing a reference frame linked to the stator flux, rotor currents will be related directly to the stator active and reactive power. An adapted control of these currents will thus permit to control the power exchanged between the stator and the grid. If the stator flux is linked to the d-axis of the frame we have:

$$\psi_{ds} = \psi_s \quad \text{and} \quad \psi_{qs} = 0 \quad (4)$$

And the electromagnetic torque can then be expressed as :

$$C_{em} = -p\frac{M}{L_s}I_{qr}\psi_{ds} \quad (5)$$

By substituting Eq.4 in Eq.1, the following rotor flux equations are obtained :

$$\begin{cases} \psi_s = L_s I_{ds} + M I_{dr} \\ 0 = L_s I_{qs} + M I_{qr} \end{cases} \quad (6)$$

In addition, the stator voltage equations are reduced to:

$$\begin{cases} V_{ds} = R_s I_{ds} + \dfrac{d}{dt}\psi_s \\ V_{qs} = R_s I_{qs} + \omega_s\psi_s \end{cases} \quad (7)$$

By supposing that the electrical supply network is stable, having for simple voltage V_s, which led to a stator flux ψ_s constant. This consideration associated with Eq.5 shows that the electromagnetic torque only depends on the q-axis rotor current component. With these assumptions, the new stator voltage expressions can be written as follows:

$$\begin{cases} V_{ds} = R_s I_{ds} \\ V_{qs} = R_s I_{qs} + \omega_s\psi_s \end{cases} \quad (8)$$

Using Eq.6, a relation between the stator and rotor currents can be established :

$$\begin{cases} I_{ds} = -\dfrac{M}{L_s}I_{dr} + \dfrac{\psi_s}{L_s} \\ I_{qs} = -\dfrac{M}{L_s}I_{qr} \end{cases} \quad (9)$$

The stator active and reactive powers are written:

$$\begin{cases} P_s = V_{ds}I_{ds} + V_{qs}I_{qs} \\ Q_s = V_{qs}I_{ds} - V_{ds}I_{qs} \end{cases} \quad (10)$$

By using Eqs.1, 4, 9 and 10, the stator active and reactive powers, the rotor fluxes and voltages can be written versus rotor currents as:

$$\begin{cases} P_s = \dfrac{\omega_s\psi_s M}{L_s}I_{qr} - \dfrac{V_s^2}{R_s} + \dfrac{\omega_s^2\psi_s^2}{R_s} \\ Q_s = -\dfrac{\omega_s\psi_s M}{L_s}I_{dr} + \dfrac{\omega_s\psi_s^2}{L_s} \end{cases} \quad (11)$$

$$\begin{cases} \psi_{dr} = (L_r - \dfrac{M^2}{L_s})I_{dr} + \dfrac{M\psi_s}{L_s} \\ \psi_{qr} = (L_r - \dfrac{M^2}{L_s})I_{qr} \end{cases} \quad (12)$$

$$\begin{cases} V_{dr} = R_r I_{dr} + (L_r - \dfrac{M^2}{L_s})\dfrac{dI_{dr}}{dt} - S\omega_s(L_r - \dfrac{M^2}{L_s})I_{qr} \\ V_{qr} = R_r I_{qr} + (L_r - \dfrac{M^2}{L_s})\dfrac{dI_{qr}}{dt} + S\omega_s(L_r - \dfrac{M^2}{L_s})I_{dr} + S\omega_s\dfrac{M\psi_s}{L_s} \end{cases} \quad (13)$$

In steady state, the second derivative terms of the two equations in 13 are equal to zero. We can thus write:

$$\begin{cases} V_{dr} = R_r I_{dr} - S\omega_s(L_r - \frac{M^2}{L_s})I_{qr} \\ V_{qr} = R_r I_{qr} + S\omega_s(L_r - \frac{M^2}{L_s})I_{dr} + S\omega_s \frac{M\psi_s}{L_s} \end{cases} \quad (14)$$

The third term, which constitutes cross-coupling terms, can be neglected because of their small influence. These terms can be compensated by an adequate synthesis of the regulators in the control loops.

4. Controllers synthesis

In this section, we have chosen to compare the performances of the *DFIG* with three different controllers: *PI, RST* and sliding mode.

Based on relations (9), (11) and (14), the control system can be designed as shown in figure 1. The blocks R_1, R_2, R_3 and R_4 represent respectively the stator powers and the rotor currents regulators.

A. PI regulator synthesis

This controller is simple to elaborate. Figure 2 shows the block diagram of the system implemented with this controller. The terms k_p and k_i represent respectively the proportional and integral gains. The quotient *B/A* represents the transfer function to be controlled, where *A* and *B* are presently defined as follows:

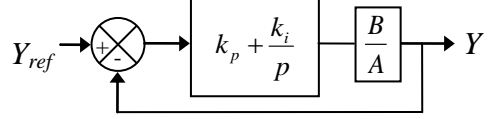$$A = L_s R_r + p.L_s\left(L_r - \frac{M^2}{L_s}\right) \text{ and } B = \omega_s\psi_s M \quad (15)$$

Fig 2. System with PI controller.

The regulator terms are calculated with a pole-compensation method. The time response of the controlled system will be fixed at 10 ms. This value is sufficient for our application and a lower value might involve transients with important overshoots. The calculated terms are:

$$k_i = \frac{1}{1\times10^{-3}}\frac{L_s R_r}{M\,\omega_s\psi_s}, \quad k_p = \frac{1}{1\times10^{-3}}\frac{L_s(L_r - \frac{M^2}{L_s})}{M\,\omega_s\psi_s} \quad (16)$$

It is important to specify that the pole-compensation is not the only method to calculate a *PI* regulator but it is simple to elaborate with a first-order transfer-function and it is sufficient in our case to compare with other regulators.

B. RST controller synthesis

The block-diagram of a system with its *RST* controller is presented on figure 3 [11].

The system with the transfer-function *B/A* has Y_{ref} as reference and is disturbed by the variable ɣ. *R, S* and *T* are polynomials which constitutes the controller. In our case, we have:

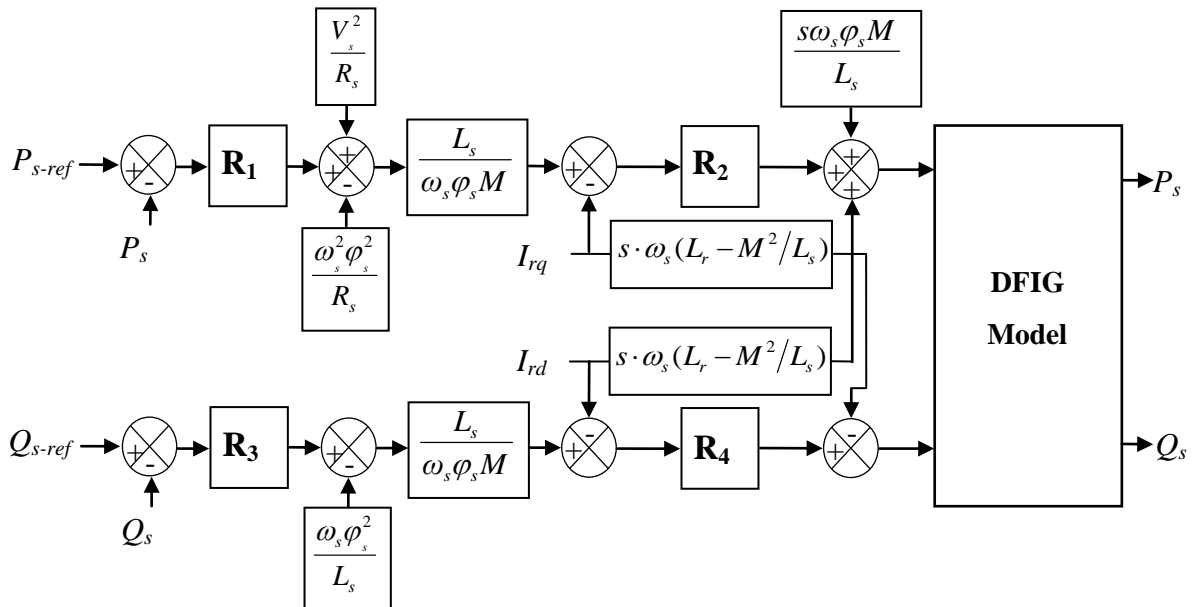$$A = L_s R_r + s \cdot L_s\left(L_r - M^2/L_s\right) \text{ and } B = MV_s \quad (17)$$
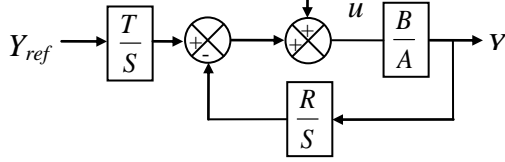
Fig 1. Power control of the DFIG.

Fig 3.Block diagram of the RST controller.

Where p is the Laplace operator.
The transfer-function of the regulated system is :

$$Y = \frac{BT}{AS + BR}Y_{ref} + \frac{BS}{AS + BR}\gamma \tag{18}$$

By applying the Besout equation, we put :

$$D = AS + BR = CF \tag{19}$$

Where C is the command polynomial and F is the filtering polynomial. In order to have good adjustment accuracy, we choose a strictly proper regulator. So if A is a polynomial of n degree $(\deg(A)=n)$ we must have :

$$\deg(D)=2n+1, \deg(S)=\deg(A)+1, \deg(R)=\deg(A)$$

In our case :

$$\begin{cases} A = a_1 p + a_0 \quad ; R = r_1 p + r_0 \\ B = b_0 \qquad\quad ; S = s_2 p^2 + s_1 p + s_0 \\ D = d_3 p^3 + d_2 p^2 + d_1 p + a_0 \end{cases} \tag{20}$$

To find the coefficients of polynomials R and S, the robust pole placement method is adopted with T_c as control horizon and T_f as filtering horizon [9]. We have:

$$p_c = -\frac{1}{T_c} \text{ and } p_f = -\frac{1}{T_f} \tag{21}$$

Where p_c is the pole of C and p_f the double pole of F. The pole pc must accelerate the system and is generally chosen three to five times greater than the pole of A $p_a.p_f$ is generally chosen three times smaller than pc. In our case:

$$T_c = \frac{1}{3}T_f = -\frac{1}{3p_a} = \frac{L_s\left(L_r - M^2/L_s\right)}{5L_s R_r} \tag{22}$$

Perturbations are generally considered as piecewise constant. γ can then be modelled by a step input. To obtain good disturbance rejections, the final value theorem indicate that the term $BS/(AS + BR)$ must tend towards zero:

$$\lim_{p \to 0} \frac{S}{D}\frac{\gamma}{p} = 0 \tag{23}$$

To obtain a good stability in steady-state, we must have $D(0){\neq}0$ and respect relation (23). The Bezout equation leads to four equations with four unknown terms where the coefficients of D are related to the coefficients of polynomials R and S by the Sylvester Matrix :

$$\begin{pmatrix} d_3 \\ d_2 \\ d_1 \\ d_0 \end{pmatrix} = \begin{pmatrix} a_1 & 0 & 0 & 0 \\ 0 & a_1 & 0 & 0 \\ 0 & 0 & b_0 & 0 \\ 0 & 0 & 0 & b_0 \end{pmatrix} \begin{pmatrix} s_2 \\ s_1 \\ r_1 \\ r_0 \end{pmatrix} \tag{24}$$

In order to determine the coefficients of T, we consider that in steady state Y must be equal to Y_{ref} so:

$$\lim_{s \to 0} \frac{BT}{AS + BR} = 1 \tag{25}$$

As we know that $S(0)=0$, we conclude that $T=R(0)$. In order to separate regulation and reference tracking, we try to make the term $BT/(AS + BR)$ only dependent on C. We then consider $T=hF$ (where h is real) and we can write:

$$\frac{BT}{AS + BR} = \frac{BT}{D} = \frac{BhF}{CF} = \frac{Bh}{D} \tag{26}$$

As $T=R(0)$, we conclude that $h = R(0)/F(0)$.

C. Super twisting sliding mode controller

The sliding mode is a technique to adjust feedback by previously defining a surface. The system which is controlled will be forced to that surface, and then the behaviour of the system slides to the desired equilibrium point [12]. The main feature of this control is that we only need to drive the error to a "switching surface". When the system is in "sliding mode", the system behaviour is not affected by any modelling uncertainties and/or disturbances. The design of the control system will be demonstrated for a nonlinear system presented in the canonical form [13]:

$$\dot{x} = f(x,t) + B(x,t)V(x,t), x \in R^n, \; V \in R^m, \; ran(B(x,t)) = m \tag{27}$$

With control in the sliding mode, the goal is to keep the system motion on the manifold S, which is defined as:

$$S = \{x : e(x, t)=0\} \tag{28}$$

$$e = x^d - x \tag{29}$$

Here e is the tracking error vector, x^d is the desired state, x is the state vector. The control input u has to guarantee that the motion of the system described in

(27) is restricted to belong to the manifold S in the state space. The sliding mode control should be chosen such that the candidate Lyapunov function satisfies the Lyapunov stability criteria :

$$\vartheta = \frac{1}{2}S(x)^2, \quad \dot{\vartheta} = S(x)\dot{S}(x). \tag{30}$$

This can be assured for:

$$\dot{\vartheta} = -\eta|S(x)| \tag{31}$$

Here η is strictly positive. Essentially, equation (30) states that the squared "distance" to the surface, measured by $e(x)^2$, decreases along all system trajectories. Therefore (31) satisfy the Lyapunov condition. With selected Lyapunov function the stability of the whole control system is guaranteed. The control function will satisfy reaching conditions in the following form:

$$V^{com} = V^{eq} + V^n \tag{32}$$

Here V^{com} is the control vector, V^{eq} is the equivalent control vector, V^n is the correction factor and must be calculated so that the stability conditions for the selected control are satisfied.

$$V^n = K \, sat((S(x)/\delta) \tag{33}$$

$sat((S(x)/\delta)$ is the proposed saturation function, δ is the boundary layer thickness. In this paper we propose the Slotine method [14]:

$$S(X) = \left(\frac{d}{dt} + \lambda\right)^{n-1} e \tag{34}$$

Here, e is the tracking error vector, λ is a positive coefficient and n is the relative degree.

In our study, we choose the error between the measured and references stator powers as sliding mode surfaces, so we can write the following expression:

$$\begin{cases} S_d = P_{S-ref} - P_S \\ S_q = Q_{S-ref} - Q_S \end{cases} \tag{35}$$

The first order derivate of (35), gives :

$$\begin{cases} \dot{S}_d = \dot{P}_{S-ref} - \dot{P}_S \\ \dot{S}_q = \dot{Q}_{S-ref} - \dot{Q}_S \end{cases} \tag{36}$$

Replacing the powers in (36) by their expressions given in (11), one obtains [15]:

$$\begin{cases} \dot{S}_d = \dot{P}_{S-ref} - \dfrac{\omega_s \psi_s M}{L_s} \dot{I}_{qr} \\ \dot{S}_q = \dot{Q}_{S-ref} + \dfrac{\omega_s \psi_s M}{L_s} \dot{I}_{dr} - \dfrac{\omega_s \psi_s^2}{L_s} \end{cases} \tag{37}$$

V_{dr} and V_{qr} will be the two components of the control vector used to constraint the system to converge to $S_{dq}=0$. The control vector V_{dqeq} is obtained by imposing $\dot{S}_{dq}=0$ so the equivalent control components are given by the following relation :

$$V_{eqdq} = \begin{bmatrix} -\dfrac{L_s\left(L_r - \dfrac{M^2}{L_s}\right)}{\omega_s \psi_s M} \dot{Q}_s^* + R_r I_{dr} - \left(L_r - \dfrac{M^2}{L_s}\right) g\omega_s I_{qr} + \dfrac{\left(L_r - \dfrac{M^2}{L_s}\right)\psi_s}{M} \\ \dfrac{L_s}{\omega_s \psi_s M} \dot{P}_s^* + R_r I_{qr} - \left(L_r - \dfrac{M^2}{L_s}\right) g\omega_s I_{dr} + \dfrac{g\omega_s \psi_s M}{L_s} \end{bmatrix} \tag{38}$$

To obtain good performances, dynamic and commutations around the surfaces, the control vector is imposed as follows :

$$V_{dq} = V_{eqdq} + K \cdot sat(S_{dq}) \tag{39}$$

The sliding mode will exist only if the following condition is met :

$$S \cdot \dot{S} < 0 \tag{40}$$

Sliding mode control (SMC) is one of the most interesting nonlinear control approaches. Nevertheless, a few drawbacks arise in its practical implementation, such as chattering phenomenon and undesirable mechanical effort. In order to reduce the effects of these problems, second order sliding mode seems to be a very attractive solution.

This method generalizes the essential sliding mode idea by acting on the higher order time derivatives of the sliding manifold, instead of influencing the first time derivative as it is the case in SMC, therefore reducing chattering and avoiding strong mechanical efforts while preserving SMC advantages [16].

In order to ensure the stator active and reactive powers convergence to their references, a super twisting sliding mode control (STSMC) is used. Considering the sliding mode surfaces given by (24), the following expression can be written :

$$\begin{cases} \dot{S}_d = \dot{P}_{S-ref} - \dfrac{\omega_s \psi_s M}{L_s} \dot{I}_{qr} \\ \ddot{S}_d = Y_1(t,x) + \Lambda_1(t,x)V_{dr} \end{cases} \tag{42}$$

And

$$\begin{cases} \dot{S}_q = \dot{Q}_{S-ref} + \dfrac{\omega_s \psi_s M}{L_s} \dot{I}_{dr} - \dfrac{\omega_s \psi_s{}^2}{L_s} \\ \ddot{S}_q = Y_2(t,x) + \Lambda_2(t,x) V_{dr} \end{cases} \qquad (43)$$

Where $Y_1(t,x)$, $Y_2(t,x)$, $\Lambda_1(t,x)$ and $\Lambda_2(t,x)$ are uncertain functions which satisfy:

$$\begin{cases} Y_1 > 0, \ |Y_1| > \lambda_1, \ 0 < K_{m1} < \Lambda_1 < K_{M1} \\ Y_2 > 0, \ |Y_2| > \lambda_2, \ 0 < K_{m2} < \Lambda_2 < K_{M2} \end{cases}$$

Basing on the super twisting algorithm introduced by Levant in [17], the proposed high order sliding mode controller contains two parts :

$$V_{dr} = v_1 + v_2 \qquad (44)$$

With

$$\dot{v}_1 = -k_1 sign(S_d)$$

$$v_2 = -l_1 |S_d|^\gamma sign(S_d)$$

$$V_{dr} = w_1 + w_2 \qquad (45)$$

With

$$\dot{w}_1 = -k_2 sign(S_q)$$

$$w_2 = -l_2 |S_q|^\gamma sign(S_q)$$

In order to ensure the convergence of the sliding manifolds to zero in finite time, the gains can be chosen as follows [17,18].

$$\begin{cases} k_i > \dfrac{\lambda_i}{K_{mi}} \\ l_i^2 \geq \dfrac{4\lambda_i}{K_{mi}^2} \dfrac{K_{Mi}(k_i + \lambda_i)}{K_{mi}(k_i - \lambda_i)} ; \ i = 1, \ 2 \\ 0 < \gamma \leq 0.5 \end{cases}$$

5. Simulation results and discussions

In this section, simulations are realized with a 2 MW generator coupled to a 690V/50Hz grid. Parameters of the machine are given in table 1. In the aim to evaluate the performances of the three controllers, three categories of tests have been realized: pursuit test, sensitivity to the speed variation and robustness against machine parameter variations.

A. Pursuit test

This test has for goal the study of the three controller's behaviours in reference tracking, while

Table 1. MACHINE PARAMETERS.

Parameters	Value	IS-Unit
Nominal power	2	MW
Stator voltage	690	V
Stator frequency	50	Hz
Number of pairs poles	2	
Stator resistance	2.6	mΩ
Rotor resistance	2.9	mΩ
Stator inductance	77.306	μH
Rotor inductance	83.369	μH
Mutual inductance	2.5	mH

the machine's speed is considered constant at its nominal value. The simulation results are presented in figure 4. As it's shown by this figure, for the three controllers, the active and reactive generated powers track their references. In addition and contrary to the PI and RST controllers where the coupling effect between the two axes is clear, we can notice that the STSMC controller ensures a perfect decoupling between them. Therefore we can consider that this controller has a good performance for this test.

B. Sensitivity to the speed variation

The aim of this test is to analyze the influence of a speed variation of the DFIG on active and reactive powers for the three controllers. For this objective and at time = 3sec, the speed was varied from 150 rad/s to 170 rad/s (Figure 5). The simulation results are shown in figure 6. This figure express that the speed variation produced a slight effect on the power curves of the three controllers. This result is attractive for wind energy applications to ensure stability and quality of the generated power when the speed is varying.

C. Robustness

In order to test the robustness of the used controllers, the stator and the rotor resistances R_s and R_r are doubled and the values of inductances L_s, L_r and M are divided by 2. The machine is running at its nominal speed. The results presented in figure 7 show that the parameters variations of the DFIG increase slightly the time-response of the RST controller. On the other hand this results show that parameter variations of the DFIG presents a clear effect on the power curves (their errors curves) and that the effect appears more significant for PI and RST controllers than that with STSMC one. Thus it can be concluded that this last is the most robust among the proposed controllers studied in this work.

6. Conclusion

The modelling, the control and the simulation of an electrical power electromechanical conversion system based on the doubly fed induction generator (DFIG) connected directly to the grid by the stator and fed by a power converter on the rotor side has been presented in this study. Our objective was the implementation of a robust decoupled control system of active and reactive powers generated by the stator side of the DFIG, in order to ensure of the high performance and a better execution of the DFIG, and to make the system insensible with the external disturbances and the parametric variations. In the first step, we started with a study of modelling on the doubly fed induction generator.

In second step, we adopted a vector control strategy in order to control the stator active and reactive powers exchanged between the DFIG and
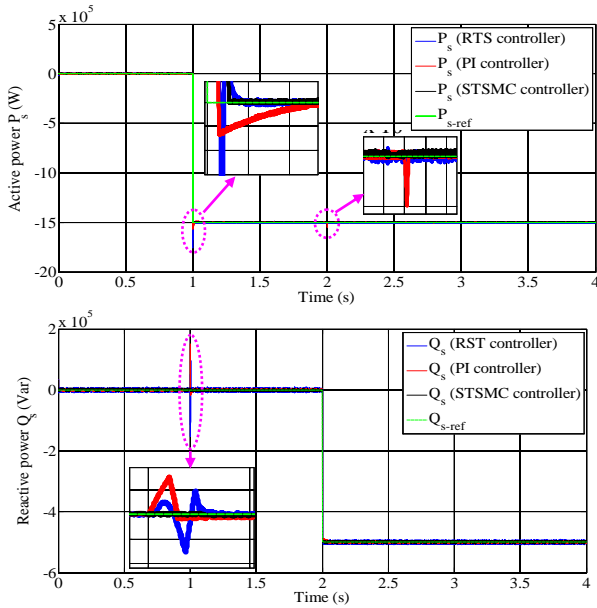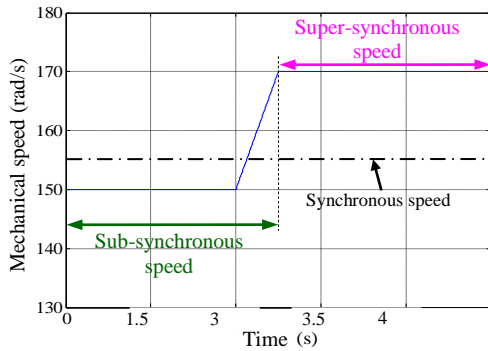
Fig 4. Reference tracking.

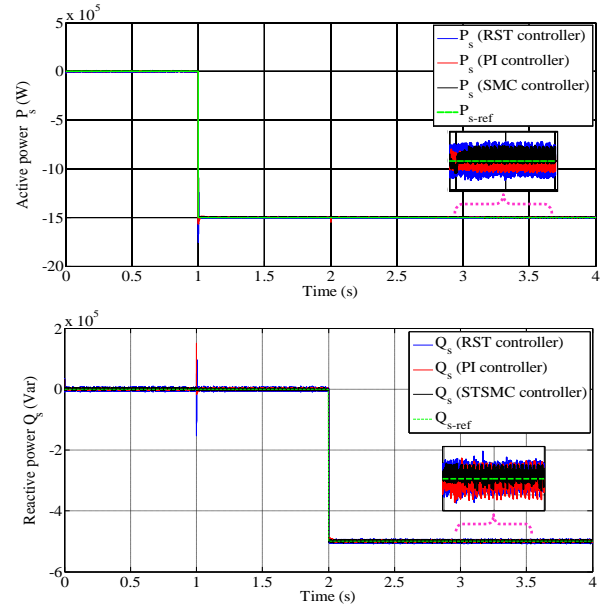Fig 5. Mechanical speed profile.
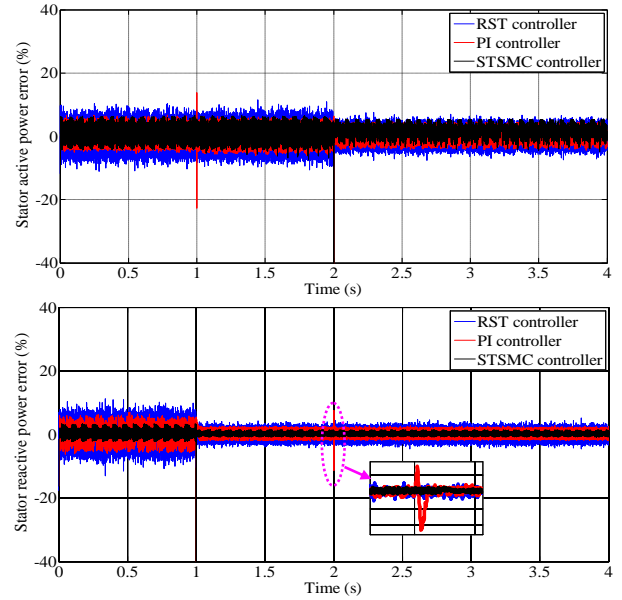
Fig 6. Sensitivity to the speed variation.

Fig 7. Sensitivity to the DFIG's parameters variation on the DFIG control.

the grid. Contrary to the previous work carried out on the DFIG where the researchers always neglect the stator resistance to facilitate its control, in our work this resistance was not neglected in order to return the system studied near to reality. In third step, three different controllers are synthesized and compared. In term of power reference tracking with the DFIG in ideal conditions (no parameters variations and no disturbances), the RST and STSMC controllers ensure a perfect decoupling between the two axes

comparatively to the PI one where the coupling effect between them is very clear.

When the machine's speed is modified (which represents a perturbation for the system), the impact on the active and reactive power values is almost negligible for the three controllers. A robustness test has also been investigated where the machine parameters have been modified. These changes induce some disturbances on the power responses but with an effect almost doubled with the PI and RST controllers than on that with STSMC one.

Basing on all these results it can be concluded that robust control method as STSMC can be a very attractive solution for devices using DFIG such as wind energy conversion systems.

References

1. Anaya-Lara,O., Jenkins,N., Ekanayake,J., Cartwright, P., Hughes,M. :*Wind Energy Generation*. In : Wiley, 2009.
2. Pena, R., Clare, J. C., Asher, G. M. :*A doubly fed induction generator using back to back converters supplying an isolated load from a variable speed wind turbine.* In: IEE Proceeding on Electrical Power Applications 143, pp. 380-387 , September 5, 1996.
3. Wu, F., Zhang, X. P., Ju, P. and Sterling, M. J. H.: *Decentralized Nonlinear Control of Wind TurbineWith Doubly Fed Induction Generator.* In : IEEE TRANS ON POWER SYSTEMS, VOL. 23, NO. 2, pp. 613-621, MAY 2008.
4. Poller, M. A. ;*Doubly-fed induction machine models for stability assessment of wind farms.* In: Power Tech Conference Proceedings, 2003, IEEE, Bologna, vol. 3, 23–26, June 2003.
5. Brekken, T., Mohan, N. :*A novel doubly-fed induction wind generator control scheme for reactive power control and torque pulsation compensation under unbalanced grid voltage conditions.* In: IEEE 34th Annual Power Electronics Specialist Conference, 2003, PESC'03, vol. 2, pp. 760-764,15-19 June 2003.
6. Brekken, T. K. A., Mohan, N. :*Control of a doubly fed induction wind generator under unbalanced grid voltage conditions.* In: IEEE Transaction on Energy Conversion, 22 March, 2007 129–135.
7. Lopez, J., Sanchis, P., Roboam, X., Marroyo, L. :*Dynamic behavior of the doubly fed induction generator during three-phase voltage dips*: In: IEEE Transaction on Energy Conversion, pp.709-717 , 22 September, 2007, 709–717.
8. Sun, T., Chen, Z., Blaabjerg, F. :*Flicker study on variable speed wind turbines with doubly fed induction generators.*In: EEE Transactions on Energy Conversion,pp. 896-905 , 20 December, 2005, 896–905.
9. Boudjema, Z., Meroufel, A. and Amari, A. :*Robust Control of a Doubly Fed Induction Generator (DFIG) Fedby a Direct AC-AC Converter*. Przegląd Elektrotechniczny, R. 88 NR 12a/2012, 213-221.
10. Hailiang ,Xu., Jiabing ,Hu. and Yikang ,He.: *Operation of Wind-Turbine-Driven DFIG Systems Under Distorted Grid Voltage Conditions*: Analysis and Experimental Validations.In: IEEE TRANSACTIONS ON POWER ELECTRONICS, VOL. 27, NO. pp. 2354-2366. 5, MAY 2012.
11. Poitier, F., Bouaouiche, T. and Machoum, M. :*Advanced control of a doubly-fed induction generator for wind energy conversion*. Electric Power Systems Research 79 (2009) 1085–1096.
12. Wai, R. J., and Chang, J. M.: *Implementation of robust wavelet-neural-network sliding-mode control for induction servo motor drive*. In: IEEE Trans. On Industrial Electronics, Vol. 50, No. 6, pp. 1317-1334, December 2003.
13. Sun, T., Chen, Z., Blaabjerg, F.: *Flicker study on variable speed wind turbines with doubly fed induction generators*. In: IEEE Transactions on Energy Conversion, pp. 896–905, 20 (December (4)) 2005.
14. Slotine, J. J. E. and Li, W. *Applied Nonlinear Control*. Englewood Cliffs, NJ: Prentice–Hall, 1991.
15. Boudjema, Z. Meroufel, A. Bounadja, E. and Djerriri, Y.: *Nonlinear control of a doubly fed induction generator supplied by a matrix converter for wind energy conversion systems*. In: Journal of Electrical Engineering, Vol. 13, No. 4, pp. 269–276, 2013.
16. Morsy, M. A. A., Said, M., Moteleb, A., Dorrah, H., T.: *Design and implementation of fuzzy sliding mode controller for switched reluctance motor*. In: Proceedings of the International MultiConference of Engineers and Computer Scientists, Vol. 2, IMECS, Hong Kong, 19-21 March 2008.
17. Levant, A., Alelishvili, L.: *Integral high-order sliding modes*. In : IEEE Trans. Autom. Control, Vol. 52, No. 7, pp. 1278-1282, July 2007.
18. Benelghali, S., Benbouzid, M. E. H., Charpentier, J. F., Ahmed-Ali, T. and Munteanu, I.: *Experimental validation of a marine current turbine simulator: Application to a PMSG-based system second-order sliding mode control*. In: IEEE Trans. Ind. Electron., Vol. 58, No. 1, pp. 118-126, January 2011.